



## **EFFECT OF NAPHTHALENE-1-YL-THIOPHENE-2-YLMETHYLENE-AMINE ON THE CORROSION INHIBITION OF MAGNESIUM ALLOYS**

**S. THIRUGNASELVI<sup>a</sup> and S. KUTTIRANI<sup>\*,b</sup>**

<sup>a</sup>Department of Chemistry, Sri Ramanujar Engineering College, CHENNAI – 600 048 (T.N.) INDIA

<sup>b</sup>Department of Chemistry, BS Abdur Rahman University, CHENNAI – 600 048 (T.N.) INDIA

### **ABSTRACT**

The inhibition effect of a Schiff base compound naphthalene-1-yl-thiophene-2-ylmethylene-amine (NT) with nitrogen and sulphur donors on AZ31 magnesium alloy corrosion was studied using weight loss method, potentiodynamic polarization and EIS (Electrochemical impedance spectroscopy). The surface characterization and its spectral analysis were exhibited using scanning electron microscopy. The results of electrochemical measurements were in good agreement with surface characterization results. It was also found that this inhibitor mainly acts through physical adsorption on the metal surface due to the presence of heteroatomic donors. Also, adsorption obeys the Freundlich isotherm. EDS spectra revealed that the existence of inhibitive layer was enriched with sulphate.

**Key words:** Magnesium, EIS, Polarization, SEM, Weight loss, Acid inhibition.

### **INTRODUCTION**

Inhibitor is a chemical additive that can effectively inhibit the corrosion of a metal in a corrosive environment with a small amount of addition. Inhibition is one of the most practical methods of protecting conventional metals from corrosion attack<sup>1</sup>. Compared with other anti-corrosion technologies, inhibition has some obvious advantages, such as no requirement of special equipment, simple control, low price and easy operation. However, the application of inhibitors in corrosion protection of magnesium alloy is not widespread today. This is because magnesium alloys are much more chemically active than conventional metals and there is lack of highly effective inhibitors for them<sup>2</sup>.

It is well known that inhibitors can be divided into passivation, precipitation and adsorption groups according to their inhibition mechanisms<sup>3</sup>. The passivating inhibitors have

---

\* Author for correspondence; E-mail: [tgchemistry@gmail.com](mailto:tgchemistry@gmail.com), [tgselvi2015@gmail.com](mailto:tgselvi2015@gmail.com)

a better protective effect on iron family metals by forming a passive film on their surfaces. However, they have an insignificant inhibition effect on non-ferrous metal, such as zinc and magnesium<sup>4</sup>. Recently, due to the demand for application of Mg alloys in some specific environments, e.g., Mg engine blocks, the use of inhibitors to protect magnesium alloys from corrosion has gradually become an important topic in Mg corrosion science.

Magnesium (Mg) alloys are one of the lightest metallic alloys currently being investigated, because of its low density ( $1.74 \text{ g/cm}^3$ ) and high mechanical stiffness<sup>5</sup>. The mechanical benefits of magnesium, is however, contrasted by a high corrosion rate as compared to aluminium or steel. Because of magnesium's electrochemical potential, as illustrated in galvanic series, it corrodes easily in the presence of sea water. The high corrosion property of magnesium has relegated the alloy to use in areas unexposed to the atmosphere, including car seat electronic boxes and structural members. The demand for the use of magnesium alloys as structural materials in automobile industry, electronic products, vibrating plates of vibrating tests machines, automotive wheels etc., have increased in recent years<sup>6</sup>. Consequently, this investigation relates to the field of corrosion inhibition of magnesium alloys, since the magnesium alloys are highly prone to corrosion.

Organic compounds containing electronegative functional groups and  $\pi$  electrons in conjugated double or triple bonds generally exhibit good inhibitive properties by supplying electrons via the  $\pi$  orbitals. Specific interaction between functional groups and the metal surface and heteroatoms like nitrogen, oxygen and sulphur play an important role in inhibition due to the free electron pairs, they possess. When both these features combine, the increase in inhibition can be observed<sup>7</sup>. Despite large numbers of organic compounds, the choice of an appropriate inhibitor for a particular system is unfortunately limited due to the variety of corrosion systems and specificity of the inhibitor compounds.

Recent publications show increased attention to Schiff base compounds as corrosion inhibitors especially in acidic environments for various metals like steel, aluminum and copper<sup>8-12</sup>. Schiff base compounds are the condensation product of an amine and a ketone/aldehyde. The greatest advantage of many Schiff base compounds is that they can be conveniently and easily synthesized from relatively inexpensive material. Also, the reports about the corrosion inhibition of magnesium and its alloys in acidic media are very scanty<sup>13,14</sup>. Compared with inhibitor studies on conventional metals, investigations of suitable inhibitors for Mg alloys and relevant understandings of inhibition mechanisms are still very limited. The search for more suitable inhibitors will continue to be a long term effort in the field of Mg inhibition. Hence, in the present investigation, the naphthalene-1-yl-thiophene-2-ylmethylene-amine (NT), an important Schiff base containing two different

heteroatoms N and S was selected and examined for its inhibition efficiency on AZ31 magnesium alloy.

## EXPERIMENTAL

### Synthesis of naphthalene-1-yl-thiophene-2-ylmethylene-amine (NT)

99% CP grade naphthalene-1-ylamine (Surechem) and laboratory scintillation grade thiophene-2-carboxaldehyde (Rolence Pharma) were mixed together in an Erlenmeyer flask. The mixture was kept under microwave radiation for four minutes on the “M-High” setting. The product obtained was brownish in nature. The resulting solution was evaporated to remove the solvent. The product was washed several times and recrystallized from ethanol. Thin layer chromatography was used to check the purity of the compound. The yield obtained was about 87%. The chemical structure of the naphthalene-1-yl-thiophene-2-ylmethylene-amine is shown in Fig. 1.

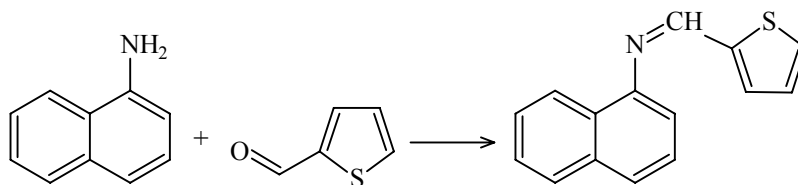


**Fig. 1: Chemical structure of the naphthalene-1-yl-thiophene-2-yl-methylene-amine**

### Elemental analysis

The Schiff base Naphthalene-1-yl-thiophene-2-ylmethylene-amine under study was identified by many techniques. The elemental analysis (CHN) is given in Table 1.

**Table 1: Elemental analysis data for CHN of Schiff base naphthalene-1-yl-thiophene-2-ylmethylene-amine**

Schiff base	Molecular weight	Percentage in mole fraction							
		C		H		N		S	
		Calc.	Found	Calc.	Found	Calc.	Found	Calc.	Found
NT	237.32	75.91	74.60	4.67	4.52	5.90	5.71	13.51	13.26
Calc.: Calculated									

## Spectral analysis

FT-IR spectra were recorded on Perkin Elmer 783 spectrophotometer by using KBr pellet. The infrared spectra are shown in Fig. 2. The peak at  $1601\text{ cm}^{-1}$  is attributed to C=O stretching vibrations and the peak at  $3045\text{ cm}^{-1}$  are related to C–H stretching vibrations in aromatic rings. Double sharp peaks at  $3300\text{--}3500\text{ cm}^{-1}$  are assigned to N–H stretching vibrations. The broad peak under other peaks at  $3400\text{--}3500\text{ cm}^{-1}$  is related to O–H stretching vibrations. The FTIR spectra of adsorbed protective layer formed on the surface was also recorded. The peaks at  $1457$  and  $1423\text{ cm}^{-1}$  are associated with the symmetric stretching vibration of C=C and the asymmetric C–N stretching vibration, respectively<sup>14</sup>. The characterized bands in the IR spectra are shown in the Table 2.

**Table 2: Characterized band of FT-IR spectra of Schiff base naphthalene-1-yl-thiophene-2-ylmethylene-amine**

Schiff base	C-H ( $\text{cm}^{-1}$ )	C=C ( $\text{cm}^{-1}$ )	O-H ( $\text{cm}^{-1}$ )	C=O ( $\text{cm}^{-1}$ )	C-N ( $\text{cm}^{-1}$ )
NT	3045	1457	3435	1601	1423

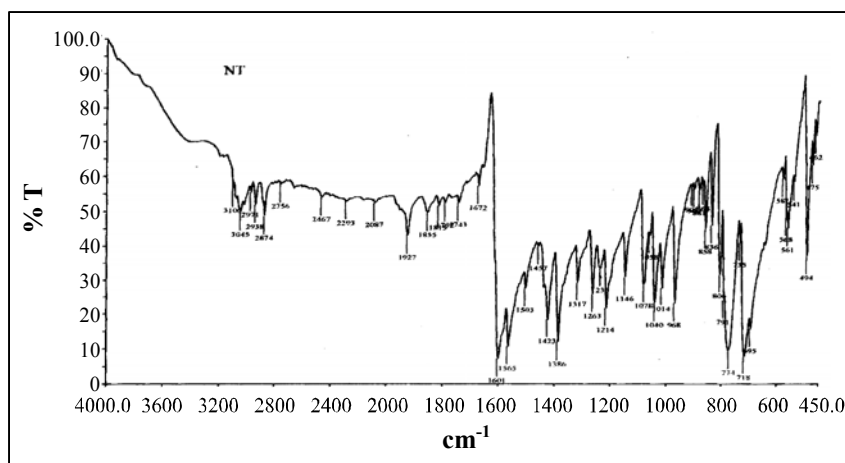


**Fig. 2: FT-IR spectrum of naphthalene-1-yl-thiophene-2-ylmethylene-amine**

## Tests materials

The material used in this study is AZ31 magnesium alloy in the form of extruded condition and supplied in plates of 6 mm thickness. The chemical composition of the AZ31 magnesium alloy consisting of Al 2.89%, 1.15% Zn, 0.2% Mn and the rest remain

magnesium. From the base metal AZ31 magnesium alloy, the corrosion tests specimens are sliced to the dimensions of 50 mm x 16 mm x 6 mm.

### Weight loss method

Solution of HCl with concentration of 0.05 mol L<sup>-1</sup> was prepared. For immersion corrosion testing, the tests method consists of immersing the specimens in an aquarium filled with HCl solution with and without inhibitor at room temperature as per ASTM G31. Prior to immersion, the magnesium alloy specimens were polished with 4/0, 3/0, 2/0 and 1/0 grade emery papers, washed thoroughly with doubly distilled water, degreased with acetone and finally dried in air. The corrosion rate of the AZ31 magnesium alloy specimen was estimated by weight loss measurement. The original weight ( $w_0$ ) of the specimen was recorded before immersion and then the specimen was immersed in the solution of HCl with and without inhibitor for immersion time of 24 hrs.

The corrosion products were removed by immersing the specimens for one min in a solution prepared by using 50 g chromium trioxide (CrO<sub>3</sub>), 2.5 g silver nitrate (AgNO<sub>3</sub>) and 5 g barium nitrate (Ba(NO<sub>3</sub>)<sub>2</sub>) in 250 mL distilled water. Finally, the specimens were washed with distilled water, dried and weighed again to obtain the final weight ( $w_1$ ). The weight loss ( $w$ ) can be measured using the following relation,

$$w = (w_0 - w_1) \quad \dots(1)$$

where,  $w$  = Weight loss in g,

$w_0$  = Original weight before tests in g, and

$w_1$  = Final weight after tests in g.

The percentage inhibition efficiency and surface coverage was calculated for the various inhibitor concentrations using the following formulae<sup>15</sup>;

$$\text{Inhibition efficiency, } \eta_w = [(W_{\text{uninhibited}} - W_{\text{inhibited}})/W_{\text{uninhibited}}] \times 100 \quad \dots(2)$$

$$\text{Surface coverage, } \theta_w = [(W_{\text{uninhibited}} - W_{\text{inhibited}})/W_{\text{uninhibited}}] \quad \dots(3)$$

Where,  $W_{\text{uninhibited}}$  – Weight loss without inhibitor (blank) in g

$W_{\text{inhibited}}$  – Weight loss with inhibitor in g

## Electrochemical methods

### Potentiodynamic polarization method

Electrochemical measurements were conducted using a Gamry AC Potentiostat Electrochemical Workstation with a three-electrode cell arrangement at room temperature. AZ31 magnesium alloy was used as a working electrode (WE) and a platinum wire was fabricated as a counter electrode (CE). Testing electrolyte of 0.05 mol L<sup>-1</sup> HCl acidic solutions was prepared with and without corrosion inhibitors. All the reported potentials were referred to the saturated calomel electrode (SCE). The potentiodynamic polarization curves were obtained by using a sweep rate of 2 mVs<sup>-1</sup> in the potential range of ± 2000 mV versus the open circuit potential. The corrosion current densities were determined using the Stern Geary equation;

$$I_{\text{corr}} = (\beta_a \times \beta_c) / 2.303 R_p (\beta_a + \beta_c) \quad \dots(4)$$

Where,  $\beta_a$  x  $\beta_c$  are the anodic and cathodic Tafel slopes, respectively.

The calculated inhibition efficiency from potentiodynamic polarization tests,  $\eta_p$  (%) is also calculated from the following equation<sup>16</sup>:

$$\text{Inhibition efficiency, } \eta_p = [(I_{\text{corr\_uninhibited}} - I_{\text{corr\_inhibited}}) / I_{\text{corr\_uninhibited}}] \times 100 \quad \dots(5)$$

$$\text{Surface coverage, } \theta_p = [(I_{\text{corr\_uninhibited}} - I_{\text{corr\_inhibited}}) / I_{\text{corr\_uninhibited}}] \quad \dots(6)$$

Where,  $I_{\text{corr\_uninhibited}}$  – Corrosion current density without inhibitor (blank) in mA cm<sup>-2</sup>

$I_{\text{corr\_inhibited}}$  – Corrosion current density with inhibitor in mAcm<sup>-2</sup>

In order to determine the polarization resistance,  $R_p$ , the potential of the working electrode was ramped ± 10 mV near  $E_{\text{corr}}$  at a scan rate of 0.1 mV s<sup>-1</sup>. Polarization resistance values were determined from the slope of the potential-current lines. The  $R_p$  values were used to calculate the inhibition efficiencies, ( $\eta_{\text{PR}}$ %), using the relation<sup>17</sup>;

$$\text{Inhibition efficiency, } \eta_{\text{PR}} = [(R_p' - R_p) / R_p'] \times 100 \quad \dots(7)$$

$$\text{Surface coverage, } \theta_{\text{PR}} = [(R_p' - R_p) / R_p'] \quad \dots(8)$$

Where,  $R_p'$  and  $R_p$  are the polarization resistances in the presence and absence of the organic additives, respectively.

## Electrochemical impedance spectroscopy

In the EIS experiments, the measured frequency range was 1-10 MHz at the open circuit potential by applying 10 mV sine wave AC voltage. All the measurements were repeated three times to check the reproducibility and the impedance data was analyzed using the ZSimpWin 3.00 software (EG&G, USA). Since  $R_p$  is inversely proportional to the corrosion current, it can be used to calculate the inhibitor efficiency ( $\eta_{EIS}$ ), from the relation<sup>20</sup>;

$$\text{Inhibition efficiency, } \eta_{EIS} = [(R_{total}' - R_{total})/R_{total}'] \times 100 \quad \dots(9)$$

$$\text{Surface coverage, } \theta_{EIS} = [(R_{total}' - R_{total})/R_{total}'] \quad \dots(10)$$

Where,  $R_{total}'$  and  $R_{total}$  are the total resistances ( $R_{ad} + R_{ct} + R_f$ ) with and without the additives, respectively.

All electrochemical testing were carried out at room temperature under ambient pressure without stirring. The volume of corrosive solution for each tests was 250 mL. The polarization and EIS results were reported for triplicate tested sample in each inhibitor concentration and the average statistical results were reported.

## RESULTS AND DISCUSSION

### Weight loss method

The average weight loss data obtained for the AZ31 magnesium alloy specimen in triplicates for various concentrations of inhibitor naphthalene-1-yl-thiophene-2-ylmethylene-amine are presented in Table 3.

**Table 3: Inhibition efficiency of the naphthalene-1-yl-thiophene-2-ylmethylene-amine for AZ31 magnesium alloy in 0.05 mol L<sup>-1</sup> HCl solution**

Inhibitor concentration (mmol L <sup>-1</sup> )	Weight loss (g)	Inhibitor efficiency (%)	Degree of surface coverage ( $\theta$ )
Blank	1.2	-	-
2.5	0.953	20.5	0.205
5	0.735	38.75	0.3875
7.5	0.671	44.08	0.4408
10	0.418	65.16	0.6516

From weight loss data obtained by performing the experiment in triplicate with the data variation of 0.5 mg, it is clear that the loss in weight of magnesium alloy specimens decreased with the increasing inhibitor concentration. Furthermore, it was found that the corrosion rate was linearly proportional to the weight loss. This means, the corrosion rate decreased with the increase in concentration of the inhibitors as shown in Table 3.

The results indicate that the weight of magnesium alloy sample decreases while comparing with the absence of Schiff bases [inhibitor] because the Schiff base forms a preventive layer on the metal surface due to azomethine group (-CH=N-) and aromatic cycles of the Schiff bases.

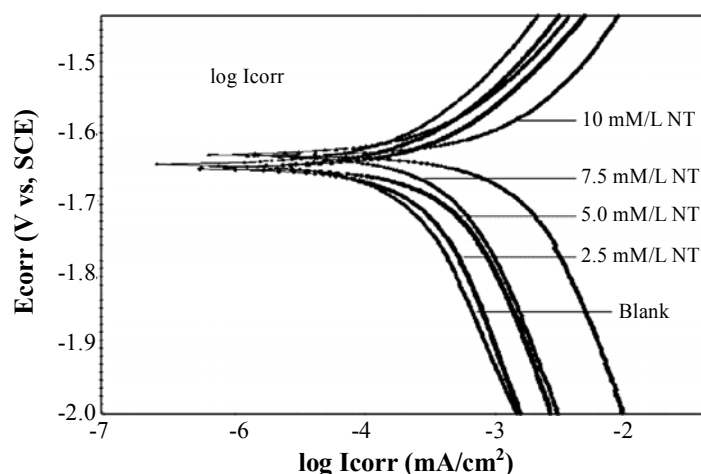
### Potentiodynamic polarization method

Fig. 3 represents the potentiodynamic polarization curves of AZ31 magnesium alloy in 0.05 M HCl in the presence and absence of various concentrations of NT Schiff base. As can be seen that the anodic and cathodic currents both decrease after addition of the Schiff base to the corrosive solution. This result suggests that the addition of the NT Schiff base reduces anodic dissolution and also retards the hydrogen evolution reaction. The values of corrosion potential ( $E_{\text{corr}}$ ) in the absence and presence of inhibitor at different concentrations are given in Table 4.

**Table 4: Polarization parameters for AZ31 magnesium alloy in 0.05 mol L<sup>-1</sup> HCl in the absence and presence of the naphthalene-1-yl-thiophene-2-ylmethylene-amine at different inhibitor concentrations**

Inhibitor conc. (mM)	$R_p$ ( $\Omega \cdot \text{cm}^2$ )	$\beta_a$ ( $\text{mV dec}^{-1}$ )	$\beta_c$ ( $\text{mV dec}^{-1}$ )	$I_{\text{corr}}$ ( $\mu\text{A cm}^{-2}$ )	$E_{\text{corr}}$ (V vs. SCE)	Inhibition efficiency (%)	
						Based on $I_{\text{corr}}$	Based on $R_p$
Blank	447.6	142	163	71.46	-1.634	-	-
2.5	626.8	144	167	51.52	-1.638	27.90	28.58
5.0	1058.2	148	161	31.44	-1.632	56.00	57.70
7.5	1615.9	145	166	20.01	-1.629	72.30	72.00
10.0	4680.4	149	169	7.14	-1.624	91.00	91.43

It is clearly seen that the corrosion potential values were shifted to more positive values in the presence of NT. Generally, if the displacement in  $E_{\text{corr}}$  after addition of inhibitor is bigger than 85 mV, the inhibitor can be classified as a cathodic or anodic type; and if the displacement is less than 85 mV, the inhibitor can be considered as mixed type<sup>18,19</sup>. In this study, the maximum displacement in  $E_{\text{corr}}$  value was lower than 85 mV towards anodic region, which indicates that the NT acts as a mixed type inhibitor. Other electrochemical corrosion parameters such as cathodic and anodic Tafel slopes ( $\beta_c$  and  $\beta_a$ ), polarization resistance ( $R_p$ ) and corrosion current density ( $I_{\text{corr}}$ ) were also obtained from polarization curves and are shown in Table 4. The values of anodic and cathodic Tafel slopes were calculated from linear region of the polarization curves. There were no significant changes in the cathodic and anodic Tafel slopes after the addition of Schiff base compound. The values tend to be more consistent along its slope. This means that the studied compound cannot change the mechanism of magnesium dissolution or hydrogen evolution.



**Fig. 3: Potentiodynamic polarization curves of AZ31 magnesium alloy in  $0.05 \text{ mol L}^{-1}$  HCl in the presence and absence of various concentrations of naphthalene-1-yl-thiophene-2-ylmethylene-amine**

### Electrochemical impedance spectroscopy

The Nyquist plots of magnesium in  $0.05 \text{ mol L}^{-1}$  HCl in the presence and absence of NT Schiff base compounds are also shown in Fig. 4. The capacitive loop in the high frequency region (second semicircle) is often related to the charge transfer resistance ( $R_{\text{ct}}$ ) and the double layer capacitance of the magnesium surface<sup>20,21</sup>. From the figure, it is obvious that the  $R_{\text{ct}}$  value in the corrosion potential is higher than that in the applied cathodic potential. A similar result in NaCl solution has been reported in the literature<sup>21</sup>. Also, the

presence of first capacitive loop at the highest frequencies is also observed. This capacitive loop will arise from non-Faradaic processes such as the adsorption of the hydrogen or chloride ions on magnesium surfaces. Similar behavior has been observed for magnesium or its alloys in alkali solutions<sup>21</sup>.

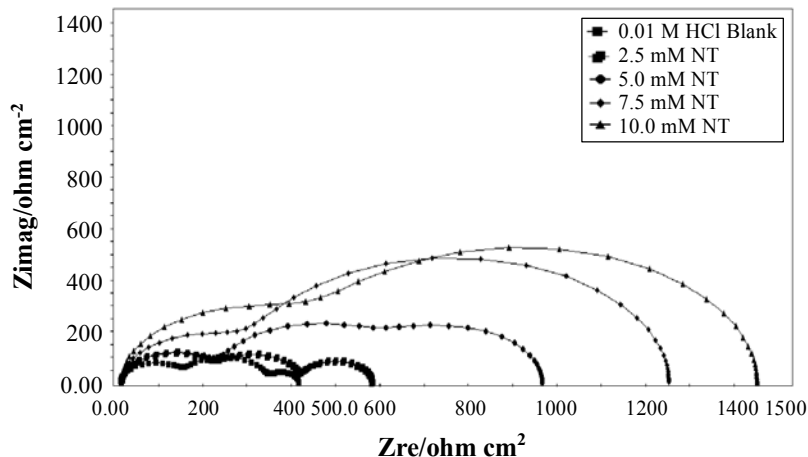


**Fig. 4:** Nyquist plots of AZ31 magnesium alloy in 0.05 M HCl in the presence and absence of various concentrations of naphthalene-1-yl-thiophene-2-ylmethylene-amine

In the case of magnesium in mild acidic solution at least two independent state variables can be distinguished. One of them is the surface coverage of the partially protective film and the other is the concentration of  $Mg^+$  ion. In Fig. 4, the inductive loop at low frequency is attributed mainly to the partially protective surface film and the third capacitive loop at medium frequencies (before the inductive loop) is related to the  $Mg^+$  ion concentration within the film free area<sup>22</sup>. These explanations are based on the partially protective surface film model. If the surface film is perfect, then these loops will not occur.

Hence, it is likely that the first capacitive loop at the highest frequencies is produced due to adsorption of hydrogen ions. This matter calls for more mechanistic studies and is beyond the aim of the present investigation. It is found that the diameter of the capacitive semicircles especially that of the second semicircle, increased with the addition of the Schiff base. This effect is more obvious in the presence of high Schiff base concentrations. This result clearly demonstrates the high inhibition performance of NT Schiff base on magnesium corrosion in acidic media.

Nyquist plots were fitted to an appropriate equivalent circuit (Fig. 5) and the relevant quantitative results were obtained. In this model,  $R_s$ ,  $R_{ct}$  and  $R_f$  characterize the solution

resistance, charge transfer resistance and partially protective film resistance respectively while the  $R_{ad}$  is inserted to account the resistance related with the first capacitive loop at highest frequencies shown in the Fig. 4. Also,  $CPE_{dl}$  and  $CPE_f$  were used to model the capacitive behaviour of the electrical double layer and partially protective film respectively. Moreover, the constant phase element  $CPE_{ad}$  was added to account for the capacitance of the first loop at highest frequencies. In the used circuit, the constant phase elements (CPE) are used instead of the ideal capacitors because the Nyquist plots contain depressed semicircles with the center under the real axis. This is the characteristic behavior of solid electrodes. In such cases, it is necessary to use constant phase elements instead of the ideal capacitors to account for the non-ideal electrodes behavior. The constant phase elements impedance can be modelled by the following equation<sup>23</sup>.

$$Z_{CPE} = [j\omega C]^{-n} \quad \dots(11)$$

where  $Z$  is the impedance,  $j$  the square root of -1,  $\omega$  the angular frequency,  $C$  the capacitance and  $n$  the measure of the non-ideality of the capacitor with a value in the range of  $1 > n > 0$ . It should be mentioned that the inductive loop elements were not entered in the circuits because the corresponding data were very scattered.

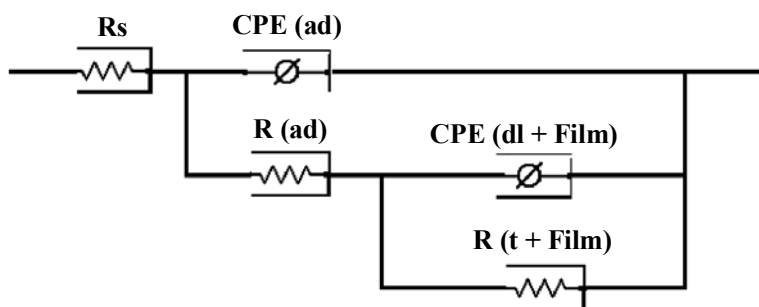


**Fig. 5: Equivalent circuit for fitting EIS data**

### Adsorption isotherm

Corrosion inhibition of AZ31 magnesium alloy in 0.05 M HCl solution by inhibitors can also be explained based on molecular adsorption. The adsorption process is influenced by the chemical structures of organic compounds, the distribution of charge in molecule, the nature and surface charge of metal and the type of aggressive media<sup>24</sup>. Basic information on the interaction between the inhibitors and the mild steel surface can be provided by the adsorption isotherms<sup>25</sup>. Totally, adsorption isotherms provide information about the interaction among the adsorbed molecules themselves and their interactions with the

electrode surface<sup>26</sup>. Schiff bases were used to tests graphically to various adsorption isotherms including Freundlich's, Langmuir, Temkin isotherms. Surface fractional coverage values were calculated based on EIS results.

To choose the suitable isotherm, the correlation coefficient ( $R^2$ ) was used and the best fit was obtained from the Freundlich's isotherm shown in Fig. 6, which can also be expressed by the following equation<sup>27,28</sup>:

$$\log \Theta = \log K + 1/n \log C \quad \dots(12)$$

where, C is the concentration of inhibitor and K is the adsorptive equilibrium constant. The parameter n is the constant describing the adsorption degree, that is, if  $0 < n < 1$ , the adsorption is easy, if  $n = 1$  the adsorption is moderate and if  $n > 1$  the adsorption is difficult. Finally, the  $\Theta$  represents the surface fractional coverage.

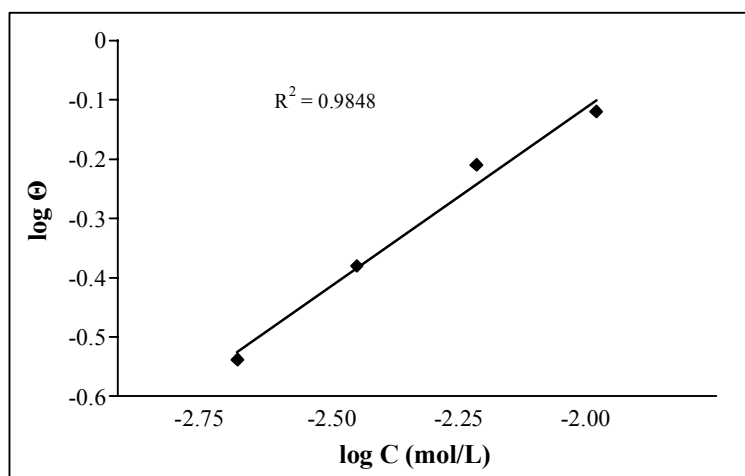


**Fig. 6: Freundlich's adsorption isotherm plot based on EIS data**

The linear relationships suggest that the adsorption of inhibitors obeys the Freundlich's adsorption isotherm. The energy of adsorption can be calculated from the following equation:

$$\Delta G_{\text{ads}} = -2.303 RT \log (55.5 K_{\text{ads}}) \quad \dots(13)$$

where, 55.5 is the molar constant of water in the solution at the temperature T is 30°C. The negative values of  $\Delta G_{\text{ads}}$  shown in the Table 6 indicate that adsorption of the inhibitors on the metal surface is spontaneous. Generally, values of  $\Delta G_{\text{ads}}$  around -20 kJmol

$L^{-1}$  or lower are consistent with the electrostatic interaction between charged molecules and the charged metal surface (physisorption); those around  $-40$  kJmol/L or higher involves charge sharing or transfer from organic molecules to the metal surface to form a coordinate type of metal bond (chemisorptions)<sup>29</sup>. These values of  $\Delta G_{ads}$  are less than  $-40$  kJmol/L and that is commonly interpreted with the presence of physical adsorption by the formation of an adsorptive film with an electrostatic character<sup>30,31</sup>.

**Table 6: Adsorption parameters for AZ31 magnesium alloy in  $0.05$  mmol  $L^{-1}$  HCl in the absence and presence of the naphthalene-1-yl-thiophene-2-ylmethylene-amine at different inhibitor concentrations**

Inhibitor conc. (mmol $L^{-1}$ )	Equilibrium constant, $K_{ads}$ (kJmol $^{-1}$ )	Free energy of adsorption $\Delta G_{ads}$ , (kJmol $^{-1}$ )
Blank	-	-
2.5	287.3	-24.12
5	571.2	-25.83
7.5	691.6	-26.30
10	974.3	-27.49

### Weight loss method

As it can be seen from the weight loss method, the inhibition efficiency (IE) increased with the increase in concentration. The inhibitor efficiency results from Table 3 show that maximum inhibition efficiency (65.16%) was observed in 10 mM concentration of the inhibitor. The degrees of surface coverage ( $\theta$ ) for different concentrations of inhibitor have been evaluated from weight loss method.

This is due to the following reason. For this inhibitor, the surface coverage increased with the increase in concentration and reached a limiting value at a higher inhibitor concentration. Correlation between  $\theta$  values and weight loss data suggest that the inhibitive action is through adsorption. In acidic solution, imine group as well as nitrogen and sulphur atoms in hetero aromatic ring can be protonated. Physical adsorption may take place due to the coordinate bond formation between electron pairs of hetero aromatic ring and metal surface can take place. Chemisorption of Schiff bases due to interaction of their  $\pi$  orbitals with metal surface occurs following deprotonisation step of the physically adsorbed protonated forms of Schiff bases<sup>18</sup>.

From the experimental and spectral evidences, it is clear that these Schiff's base compound acts as good inhibitor. The results of this study confirm that whenever two or more hetero atoms or electro active groups present enhances the inhibition nature of compound. In the examined inhibitor, the presence of nitrogen and sulphur group has contributed for the higher inhibition efficiencies.

### **Potentiodynamic polarization tests**

The addition of Schiff base during the polarization tests increases the polarization resistance of magnesium in 0.05 M HCl and this leads to a reduction in corrosion current as shown in Table 4. These results show that the used compound acts as an effective inhibitor for magnesium in the studied corrosive media. The inhibitor efficiencies increased from 28.58 (lowest) to 91.00 (highest). Increasing inhibitor concentrations decreases corrosion current densities. The presence of inhibitors resulted in a slight shift of the corrosion potential towards the active direction in comparison to the result obtained in the absence of the inhibitor. Both the anodic and cathodic current densities were decreased indicating that the inhibitors suppressed both; the anodic and cathodic reactions. This phenomenon may be due to the existence of a naphthalene ring having high electron density. On the other hand, in the presence of inhibitors both anodic and cathodic Tafel slopes almost remain unchanged, indicating that the inhibitors acted by merely blocking the reaction sites of the metal surface without changing the anodic and cathodic reaction mechanisms<sup>32,33</sup>.

### **Electrochemical impedance spectroscopy**

The fitting was carried out using *Z* view 2 software and the produced data are displayed in Table 5. As can be seen, the total resistance of the magnesium surface significantly to increase after the addition of NT Schiff base of different concentrations, implying that the Schiff base compound used acts as effective corrosion inhibitor for magnesium in the studied corrosive solution.

Also as the inhibitor concentration increases, the inhibition efficiencies increased probably due to more NT molecules adsorbed on the magnesium surface. For low inhibitor concentrations, the  $CPE_{dl}$  decreases as the inhibitor concentration increases. The decrease in  $CPE_{dl}$  was caused either by the reduction of the local dielectric constant and/or the increased electrical double layer thickness. This fact suggests that the studied inhibitor molecule acts by adsorption at the metal/solution interface<sup>34</sup>. Results obtained from EIS measurements are in good agreement with that obtained from both potentiodynamic polarization and weight loss measurements. Electrochemical impedance spectroscopy and polarization curves measurements were repeated several times and it was observed that they were highly reproducible.

**Table 5: Impedance parameters for AZ31 magnesium alloy in 0.05 mol L<sup>-1</sup> HCl in the absence and presence of the naphthalene-1-yl-thiophene-2-ylmethylene-amine at different inhibitor concentrations**

Inhibitor conc. C (mmol L <sup>-1</sup> )	Added resistance R <sub>ad</sub> (Ωcm <sup>2</sup> )	CPE <sub>ad</sub> (nFcm <sup>-2</sup> )	Charge transfer resistance R <sub>ct</sub> (Ωcm <sup>2</sup> )	CPE <sub>dl</sub> (nFcm <sup>-2</sup> )	Film resistance R <sub>f</sub> (Ωcm <sup>2</sup> )	CPE <sub>f</sub> (nFcm <sup>-2</sup> )	Total resistance R <sub>p</sub> (Ωcm <sup>2</sup> )	Inhibitor efficiency (%)
Blank	141.2	0.621	189.5	0.522	71.3	8.11	402.0	-
2.5	210.4	0.418	193.2	0.453	162.5	7.09	566.1	28.98
5	215.9	0.109	369.6	0.312	362.7	5.67	948.2	57.60
7.5	372.6	0.082	963.5	0.118	-	-	1336.1	69.91
10	978.2	0.015	2958.4	0.105	-	-	3936.72	91.97

### Adsorption isotherm

It was observed that, the inhibition of active dissolution of the metal is due to the adsorption of the inhibitor molecules on the metal surface forming a protective layer. The inhibitor molecules can be adsorbed onto the metal surface through the electron transfer from the adsorbed species to the vacant electron orbital of low-energy in the metal to form a coordinate type link.

The difference in inhibition efficiency between the concentrations lies mostly in the quantity of the organic compound; NT being larger due to the presence of a naphthalene ring and thiophene ring, and hence, more effective. Efficient adsorption is the result of  $\pi$  electrons of the aromatic system, double bonds and electronegative nitrogen atoms present in the structure. During chemisorptions of the compounds, electron transfer can be expected with compounds having relatively loosely bound electrons<sup>35</sup>. The  $\pi$  electrons in the system are then likely to be the determining factor in the adsorption process<sup>36,37</sup>.

### CONCLUSION

- (i) The Schiff base NT showed an inhibiting effect on AZ31 magnesium alloy corrosion in 0.05 M HCl solution. From weight loss measurements, it was observed that the inhibition efficiency increased with the increase of inhibitor concentration.
- (ii) Potentiodynamic polarization curves showed that AC inhibits both anodic and cathodic reactions at all concentration, which indicate it to be a mixed type inhibitor.
- (iii) EIS results indicate that as the additive concentration was increased the polarization resistance increased, whereas double-layer capacitance decreased.
- (iv) The adsorption of AC on the AZ31 magnesium alloy surface from 0.05 M HCl obeyed the Freundlich's adsorption isotherm.
- (v) The negative values of  $\Delta G_{\text{ads}}$  reveal spontaneous adsorption of inhibitor on the metal surface and point to the physical nature of the adsorption on the magnesium surface.
- (vi) Inhibition is the result of the adsorption of the compounds on the magnesium alloy surface and blocking of the active sites. The presence of N and S atoms, heterocyclic and aromatic rings, increased the inhibition effect of NT with respect to the other concentrations under investigation.

## ACKNOWLEDGEMENT

The authors are very grateful to the Department of Chemistry of Sri Ramanujar Engineering College, Chennai, BS Abdur Rahman University, Chennai and PSG College of Technology, Coimbatore to carry out this investigation successfully. The authors also acknowledge the Principal, Dean and Management of Sri Ramanujar Engineering College for their timely help rendered.

## REFERENCES

1. G. Song, An Irreversible Dipping Sealing Technique for Anodized ZE41 Mg Alloy, *Surface Coating Technol.*, **203**, 3618-3625 (2009).
2. G. Song and D. St. John, Corrosion of Magnesium Alloys in Commercial Engine Coolants, *Mater. Corrosion*, **56**, 15-23 (2005).
3. O. P. C. Kafor, M. E. Ikpi, I. E. Uwah, E. E. Ebenso, U. J. Ekpe and S. A. Umoren, Inhibitory Action of Phyllanthusamarus Extracts on the Corrosion of Mild Steel in Acidic Media, *Corrosion Sci.*, **50**, 2310-2317 (2008).
4. M. A. Amin, H. H. Hassan and S. S. Abd El Rehim, On the Role of NO<sub>2</sub> Ions in Passivity Breakdown of Zn in Deaerated Neutral Sodium Nitrite Solutions and the Effect of some Inorganic Inhibitors Potentiodynamic Polarization, Cyclicvoltammetry, SEM and EDX Studies, *Electrochim. Acta*, **53**, 2600-2609 (2008).
5. J. Hu, D. Huang, L. Song and X. Guo, The Synergistic Inhibition Effect of Organic Silicate and Inorganic Zn Salt on Corrosion of Mg-10Gd-3Y Magnesium Alloy, *Corrosion Sci.*, **53**, 4093-4101 (2011).
6. J. Zhang, Y. Chan and Q. Yu, Plasma Interface Engineered Coating Systems for Magnesium Alloys, *Prog. Org. Coatings*, **61**, 28-37 (2008).
7. A. Raman and P. Labine, Reviews on Corrosion Inhibitor Science and Technology, *Corrosion*, **1(11)**, 20-26 (1986).
8. K. C. Emregul, A. A. Akay and O. Atakol, The Corrosion Inhibition of Steel with Schiff Base Compounds in 2 M HCl, *Mater. Chem. Phys.*, **93**, 325-329 (2005).
9. K. C. Emregul and M. Hayvali, Studies on the Effect of a Newly Synthesized Schiff Base Compound from Phenazone and Vanillin on the Corrosion of Steel in 2 M HCl, *Corrosion Sci.*, **48**, 797-812 (2006).

10. H. Ashassi-Sorkhabi, B. Shaabani and D. Seifzadeh, Corrosion Inhibition of Mild Steel by some Schiff Base Compounds in Hydrochloric Acid, *Appl. Surface Sci.*, **23**, 154-164 (2005).
11. M. Ehteshamzade, T. Shahrabi and M. G. Hosseini, Inhibition of Copper Corrosion by Self-assembled Films of New Schiff Bases and their Modification with Alkanethiols in Aqueous Medium, *Appl. Surface Sci.*, **252**, 2949-2959 (2006).
12. G. Williams, H. N. McMurray and R. Grace, Inhibition of Magnesium Localised Corrosion in Chloride Containing Electrolyte, *Electrochim. Acta*, **55**, 7824-7833 (2010).
13. D. Seifzadeh, H. Basharnavaz and A. Beezatpour, A Schiff Base Compound as Effective Corrosion Inhibitor for Magnesium in Acidic Media, *Mater. Chem. Phys.*, **88**, 1-9 (2013).
14. A. P. Elisabete and F. M. Marina, Determination of Volatile Corrosion Inhibitors by Capillary Electrophoresis, *J. Chromatogr. A*, **1051(1-2)**, 303-308 (2004).
15. Q. M. Mohammed, Synthesis and Characterization of New Schiff Bases and Evaluation as Corrosion Inhibitors, *J. Basrah Res.*, **37**, 116-130 (2011).
16. K. F. Khaled and N. Hackerman, Investigation of the Inhibitive Effect of Ortho-Substituted Anilines on Corrosion of Iron in 1 M HCl Solutions, *Electrochim. Acta*, **48**, 2715-2723 (2003).
17. H. A. Sorkhabi and D. Seifzadeh, Analysis of Raw and Trend Removed EN Data in Time Domain to Evaluate Corrosion Inhibition Effects of New Fuchsin Dye on Steel Corrosion and Comparison of Results with EIS, *J. Appl. Electrochem.*, **38**, 1545-1552 (2008).
18. W. Li, Q. He, S. Zhang, C. Pei and B. Hou, Some New Triazole Derivatives as Inhibitors for Mild Steel Corrosion in Acidic Medium, *J. Appl. Electrochem.*, **38**, 289-295 (2008).
19. V. V. Torres, R. S. Amado, C. Faia de Sa, T. L. Fernandez, C. A. S. Riehl, A. G. Torres and E. D. Elia, Inhibitory Action of Aqueous Coffee Ground Extracts on the Corrosion of Carbon Steel in HCl Solution, *Corrosion Sci.*, **53**, 2385-2392 (2011).
20. G. Song, A. Atrens, D. St. John, Wu and J. Nairn, The Anodic Dissolution of Magnesium in Chloride and Sulphate Solutions, *Corrosion Sci.*, **39**, 1981-2004 (1997).
21. C. Chu-Nan, On the Impedance Plane Displays for Irreversible Electrode Reactions Based on the Stability Conditions of the Steady-State-II, Two State Variables Besides Electrode Potential, *Electrochim. Acta*, **35**, 837-844 (1990).

22. C. N. Cao, On the Impedance Plane Displays for Irreversible Electrode Reactions Based on the Stability Conditions of the Steady-State-I, One State Variable Besides Electrode Potential, *Electrochim. Acta*, **35**, 831-836 (1990).
23. R. Solmaza, G. Kardas, M. Culha, B. Yazici and M. Erbil, Investigation of Adsorption and Inhibitive Effect of 2-mercaptothiazoline on Corrosion of Mild Steel in Hydrochloric Acid Media, *Electrochim. Acta*, **53**, 5941-5952 (2008).
24. A. K. Maayta and N. Al-Rawashdeh, Inhibition of Acidic Corrosion of Pure Aluminum by some Organic Compounds, *Corrosion Sci.*, **46**, 1129-1140 (2004).
25. K. M. Ismail, Evaluation of Cysteine as Environmentally Friendly Corrosion Inhibitor for Copper in Neutral and Acidic Chloride Solutions, *Electrochim. Acta*, **52**, 7811-7819 (2007).
26. E. A. Noor and A. H. Al-Moubaraki, Thermodynamic Study of Metal Corrosion and Inhibitor Adsorption Processes in Mild Steel/1-methyl-4[4(-X)-styrylpyridinium iodides/ Hydrochloric Acid Systems, *Mater. Chem. Phys.*, **110**, 145-154.S (2008).
27. B. Safak, A. Duran, G. Yurt and Turkoglu, Schiff Bases as Corrosion Inhibitor for Aluminium in HCl Solution, *Corrosion Sci.*, **54**, 251-259 (2012).
28. X. Li, S. Deng and H. Fu, Sodium Molybdate as a Corrosion Inhibitor for Aluminium in H<sub>3</sub>PO<sub>4</sub> Solution, *Corrosion Sci.*, **53**, 2748-2753 (2011).
29. S. M. A. Hosseini, M. Salari, M. Ghasemi and M. Abaszadeh, Enaminone Compounds as Corrosion Inhibitors for Austenitic Stainless Steel in Sulphuric Acid Solution, *J. Phys. Chem.*, **223**, 769-777 (2009).
30. R. Solmaza, G. Kardas, M. Culha, B. Yazici and M. Erbil, Investigation of Adsorption and Inhibitive Effect of 2-mercaptothiazoline on Corrosion of Mild Steel in Hydrochloric Acid Media, *Electrochim. Acta*, **53**, 5941-5952 (2008).
31. M. Lagrenee, B. Mernari, M. Bouanis, M. Traisnel and F. Bentiss, Study of the Mechanism and Inhibiting Efficiency of 3,5-bis(4-methylthiophenyl)-4H-1,2,4-triazole on Mild Steel Corrosion in Acidic Media, *Corrosion Sci.*, **44**, 573-588 (2002).
32. H. Amar, A. Tounsi, A. Makayssi, A. Derja, J. Benzakour and A. Outzourhit, Corrosion Inhibition of Armco Iron by 2-mercaptobenzimidazole in Sodium Chloride 3% Media, *Corrosion Sci.*, **49**, 2936-2945 (2007).
33. M. A. Migahed, E. M. S. Azzam and S. M. I. Morsy, Electrochemical Behaviour of Carbon Steel in Acid Chloride Solution in the Presence of Dodecyl Cysteine Hydrochloride Self-Assembled on Gold Nanoparticles, *Corrosion Sci.*, **51**, 1636-1644 (2009).

34. H. Ashassi-Sorkhabi, B. Shaabani and D. Seifzadeh, Effect of some Pyrimidinic Schiff Bases on the Corrosion of Mild Steel in Hydrochloric Acid Solution, *Electrochim. Acta*, **50**, 3446-3452 (2005).
35. G. TrabANELLI, in: F. Mansfield, (Ed.), *Corrosion Mechanisms*, Marcel Dekker, New York (1987) p. 18.
36. I. L. Rozenfeld, *Corrosion Inhibitors*, McGraw-Hill, New York (1981) pp. 98-128.
37. T. Kristof and T. Solomon, Electrochemical Investigation of the Inhibiting Properties of 2-propyn-1-ol on Carbon Steel in Hydrochloric Acid, *Mater. Corrosion*, **41**, 519-522 (1990).
38. K. F. Khaled, The Inhibition of Benzimidazole Derivatives on Corrosion of Iron in 1 M HCl, *Electrochim. Acta*, **48**, 2493-2503 (2003).
39. A. Fekry and R. Mohamed, Acetylthiourea Chitosan as Eco-friendly for Mild Steel in Sulphuric Acid Medium, *Electrochim. Acta*, **55**, 1933-1939 (2010).
40. H. Junying, D. Huang, G. Zhang, G. Song and X. Guo, Research on the Inhibition Mechanism of Tetraphenylporphyrin on AZ91D Magnesium Alloy, *Corrosion Sci.*, **63**, 367-378 (2012).

*Accepted : 26.11.2015*